

## STATISTICAL STUDY OF INCOHERENT INTEGRATION APPLIED TO SIMULATED POWER SPECTRA OF RADAR SIGNALS BACKSCATTERED FROM EQUATORIAL ELECTROJET IRREGULARITIES

Henrique Carlotto Aveiro<sup>1</sup>, Clezio Marcos Denardini<sup>2</sup>, Mangalathayil Ali Abdu<sup>3</sup>  
and Nelson Jorge Schuch<sup>4</sup>

Recebido em 23 janeiro, 2006 / Aceito em 8 março, 2007  
Received on January 23, 2006 / Accepted on March 8, 2007

**ABSTRACT.** Spectral analysis of radar echoes through spectral moment estimation allows to identify the characteristics of plasma irregularities from equatorial electrojet. The curve fitting using the maximum likelihood estimator (MLE) was chosen as the technique to obtain the plasma irregularity information. The implication of applying distinct number of incoherent integration to simulated Type 1 plasma irregularity radar spectra is investigated. The response of the fitting is evaluated using the covariance matrix of the MLE. A statistical study of incoherent integration applied to equatorial electrojet plasma irregularity spectra is presented in order to determine its effects over the estimation of Doppler velocities. The optimal values of incoherent integrations in relation to the goodness of the fitting are obtained in order to better determine the Type 1 plasma irregularity characteristics.

**Keywords:** ionosphere, aeronomy, radar, digital signal processing, curve fitting.

**RESUMO.** A análise espectral de ecos de radar através da estimação dos momentos espectrais permite a identificação das características das irregularidades de plasma das irregularidades do eletrojato equatorial. Dentre as técnicas usadas para obtenção das informações de irregularidades de plasma, é utilizado o ajuste de curvas pela estimação de máxima verossimilhança. Este trabalho analisa a aplicação de valores distintos de integração incoerente a espectros simulados de radar de irregularidades de plasma do Tipo 1. A resposta do ajuste é avaliada utilizando a matriz de covariâncias do estimador de máxima verossimilhança. Um estudo estatístico da integração incoerente aplicado a espectros de irregularidades do EEJ é apresentado de modo a determinar seus efeitos sobre a estimação das velocidades Doppler. Os valores ótimos de integrações incoerentes em relação à qualidade do ajuste são obtidos de forma a melhor determinar as características de irregularidades de plasma do Tipo 1 do EEJ.

**Palavras-chave:** ionosfera, aeronomia, radar, processamento de sinais digitais, ajuste de curvas.

---

<sup>1</sup>Southern Regional Space Research Center, National Institute for Space Research, Av. Roraima, s/n, Bairro Camobi, P.O. Box 5021 – 97110-970 Santa Maria, RS, Brazil. Phone: +55 (55) 3220-8021; Fax: +55 (55) 3220-8007 – E-mail: aveiro@lacesm.ufsm.br

<sup>2</sup>National Institute for Space Research, Av. dos Astronautas, 1.758, Jardim da Granja, P.O. Box 515 – 12227-010 São José dos Campos, SP, Brazil. Phone: +55 (12) 3945-7156; Fax: +55 (12) 3945-6990 – E-mail: denardin@dae.inpe.br

<sup>3</sup>National Institute for Space Research, Av. dos Astronautas, 1.758, Jardim da Granja, P.O. Box 515 – 12227-010 São José dos Campos, SP, Brazil. Phone: +55 (12) 3945-7149; Fax: +55 (12) 3945-6990 – E-mail: maabdu@dae.inpe.br

<sup>4</sup>Southern Regional Space Research Center, National Institute for Space Research, Av. Roraima, s/n, Bairro Camobi, P.O. Box 5021 – 97110-970 Santa Maria, RS, Brazil. Phone: +55 (55) 3220-8021; Fax: +55 (55) 3220-8007 – E-mail: njschuch@lacesm.ufsm.br

## INTRODUCTION

The equatorial electrojet (EEJ) is an electric current that flows in the height region from about 90 to 120 km (at ionospheric E-region), covering a latitudinal range of  $\pm 3^\circ$  around the dip equator (Forbes, 1981). It is driven by the E-region dynamo electric field (Fejer & Kelley, 1980) and represents an important aspect of the phenomenology of the equatorial ionosphere-thermosphere system. Sounding observations of the equatorial ionospheric E-region using VHF radars have shown backscattered echoes from electron density irregularities in the EEJ in several sectors, such as the Peruvian sector (Cohen & Bowles, 1967; Balsley, 1969; Cohen, 1973; Fejer et al., 1975; Farley, 1985), the Indian sector (Prakash et al., 1971; Reddy & Devasia, 1981; Somayajulu et al., 1991), and the Brazilian sector (Abdu et al., 2002; Abdu et al., 2003; de Paula & Hysell, 2004; Denardini et al., 2004; Denardini et al., 2005). These echoes contain Doppler shifted frequency components due to the drift of the irregularities. The echoes present distinct spectral signatures called Type 1 and type 2 spectra. The type 1 spectrum is produced by irregularities generated by the two-stream plasma instability process (Farley, 1963; Buneman, 1963) and the type 2 is originated from the gradient drift instability mechanism (Rogister & D'Angelo, 1970). Several experiments have been conducted to investigate the EEJ irregularities in order to characterize its spectra and explain the phenomenology (Reddy, 1981; Fejer & Kelley, 1980; Forbes, 1981, and references therein).

In the Brazilian sector a 50 MHz coherent backscatter radar, also known by the acronym RESCO (in Portuguese, *Radar de Espalhamento COerente*), has been operated since 1998 at São Luís, State of Maranhão (2.33°S, 44.2°W, DIP: -0.5), on the dip equator. Observations of EEJ 3-m plasma irregularities are routinely carried out with the main purpose of studying the EEJ dynamics through spectral analysis of the backscattered echoes from plasma instabilities. For such studies, a precise determination of the spectral moments of the irregularities is a crucial requirement. Several techniques for estimating Doppler shifts based on radar power spectra have been developed and reviewed (May & Strauch, 1989; May et al., 1989; Woodman, 1985). In the present work we have estimated the irregularity Doppler shifts by fitting two Gaussians to each power spectrum using the Least Squares Fitting Method (Levenberg, 1944; Marquardt, 1963; Press et al., 1992). In this case, the quality of the fitting will depend on the variance of the noise present in the spectrum. And a well-known tool to reduce variance of the noise is the incoherent integrations, a technique

that does not change the mean spectral densities of both signal and noise. Increasing the number of integrated spectra means to reduce the variance and to define better the power spectra. In this way we have used the incoherent integration technique applied to simulated power spectra of radar signals like it was backscattered from equatorial electrojet irregularities type 1 to quantify the advantages and disadvantages of applying such technique. In the following section we present the typical radar data processing, a brief description of the spectra simulations, and the results of this statistical study, which are discussed in terms of goodness of the estimates and the variance of the estimate Doppler frequency type 1.

## RADAR DATA PROCESSING AND THE INCOHERENT INTEGRATION

The current RESCO data processing consist in fitting the sum of two Gaussians (each one representing one type of irregularity) both having a white noise level to each Doppler power spectra, which usually has an aliasing frequency of 250-500 Hz after being obtained from the Fast Fourier Transform (FFT) of the received echoes. The frequency resolution will depend upon the aliasing frequency and the number of sequential pulses. For the present study we have chosen the frequency resolution to be about 1 Hz. This processing is made based on the assumption that each spectrum is described by a S distribution in function of the frequency, given by:

$$S(f) = \frac{P_1}{\sigma_1 \sqrt{2\pi}} \exp \left[ -\frac{(f - f_{d1})^2}{2\sigma_1^2} \right] + \frac{P_2}{\sigma_2 \sqrt{2\pi}} \exp \left[ -\frac{(f - f_{d2})^2}{2\sigma_2^2} \right] + P_N, \quad (1)$$

where  $P_N$ ,  $P_i$ ,  $\sigma_i$  and  $f_{di}$  are the noise level, spectral power, spectral width and Doppler frequency, respectively. The  $i$  index indicates the type of the described irregularity: type 1 ( $i = 1$ ) or type 2 ( $i = 2$ ). The Maximum Likelihood Estimate (MLE) has been used for nonlinear fitting of the 7 parameters of each spectrum,  $\mathbf{a} = \{f_{d1}, f_{d2}, \sigma_1, \sigma_2, P_1, P_2, P_N\}$ . The fitting method is based on finding the parameters  $\mathbf{a}$  that maximize the probability function  $P(y_1 \dots y_n | \mathbf{a})$  of obtaining the data set  $y = \{y_1 \dots y_n\}$ . In other words, it is a problem of finding the parameters  $\mathbf{a}$  that minimize the square sum of residual errors between the observational data set  $y$  and the corresponding Gaussians  $S(f)$  that describes the data set, considering the uncertainty  $\sigma_i$  related to each point  $y_i$ . Eq. (2), named objective function, describes mathematically

tically the above statement.

$$\chi^2 \equiv \sum_{i=1}^N \frac{[y_i - S(f_i, P_1, f_{d1}, \sigma_1, P_2, f_{d2}, \sigma_2, P_N)]^2}{\sigma_i} \quad (2)$$

Here,  $N$  is the number of frequencies in the power spectrum,  $y_i$  is the observed spectral amplitude for a given frequency and all the other parameters have been introduced before. Despite curve fitting algorithm being largely used, it usually does not present satisfactory results when the variance is too high. One of the solutions to reduce high variances is to integrate incoherently several consecutive spectra. The method consists in averaging the power spectral density at a given frequency from several consecutive spectra, for all frequencies in the spectrum. Since the white noise is a random component, the resulting spectrum will have lower variance. Figure 1 presents an illustration of the resulting spectrum (on the right side) from incoherent integration of hundred consecutive spectra (on the left side), where a noisy bunch of spectra (represented by the first one) became a smoothed one. The incoherent integration reduces the variance of the noise ( $\sigma_{N^2}$ ) and better defines the power spectra, but it does not change the mean values of signal ( $P$ ) and noise spectral ( $P_N$ ) densities (Fukao, 1989). In a spectrum without incoherent integration,  $\sigma_N$  is equal to  $P_N$ . But, the unitary ratio  $\sigma_N/P_N$  decays with the inverse of the square root of the number of incoherent integrations ( $NICH$ ), i.e.,  $\sigma_N$  becomes equal to the relation  $P_N/(NICH)^{1/2}$ .

## SIMULATION AND PROCESSING OF POWER SPECTRA

This work focuses on the study of the effects of incoherent integration on the type 1 power spectra of backscattered signals from 3-m EEJ plasma irregularities. This class of spectrum normally presents a sharp peak centered at around 120 Hz, which corresponds to a Doppler shift of about 360 m/s (ion-acoustic speed) for radars operating at 50 MHz. So, the Gaussian covariance model of Zrnic (1979) was used to simulate groups of one thousand Gaussian like power spectra. Each power spectrum being constituted of 256 data points with typical characteristics of type 1 irregularities ( $f_d = 120$  Hz,  $\sigma = 20$  Hz). White noise was added at 6 dB signal-to-noise ratio ( $SNR$ ) in time domain in order to assure a more realistic variance in the power spectra. These groups were arranged and those spectra were integrated incoherently in such a way that we always have one thousand power spectra per group and each group represents one different value of  $NICH$ : 1, 2, 4, 6, 8, 10, 20, 40, 60, 80 and 100. In summary, Eq. (2) was simplified to a case of a single Gaussian

described by a  $S$  distribution in function of the frequency, as given per equation (3).

$$S(f) = \frac{P}{\sigma\sqrt{2\pi}} \exp\left[-\frac{(f-f_d)^2}{2\sigma^2}\right] + P_N \quad (3)$$

The quantities in this equation are the same as describe for equation 1 and refer to a type 1 Gaussian. Figure 2 presents an example of a spectrum simulated as above. The superimposed color lines (accompanied by their respective symbols) indicate the quantities mentioned in the power spectrum. The green line represents the power density of the noise ( $P_N$ ). The vertical blue line shows the center of frequency distribution ( $f_d$ ). The difference between the brown and blue vertical lines determines the standard deviation of the fitted curve. And the area between the red and the green line defines the signal power ( $P$ ).

The data sets of power spectra simulated as described here were processed as ordinary spectra obtained in the RESCO data processing. We have used MLE to minimize the square sum of residual error in a way to fit a Gaussian (Eq. 3). The same algorithm has fitted each spectrum of the eleven data set groups to a single Gaussian. And the basic analysis consisted in to compare directly the  $f_d$  fitted to the spectra using Gaussians to the *a priori*  $f_d$  value used to generate the type 1 spectra during the spectra simulation. Moreover, the goodness of the fitting was analyzed in function of the number of incoherent integrations and the variance of the estimated parameters as well.

## RESULTS AND DISCUSSIONS

The response of the method for the center of frequency distribution is shown in the Figure 3. Each histograms of the Doppler frequency distribution for Gaussian type 1 (frequency axis) is presented as a function of the number of integrations ( $NICH$  axis). Each bar of the histograms is centered in the integer frequency defined in the frequency axis with  $\pm 0.5$  Hz of resolution. For instance, the bars for 120 Hz represent the density of answers of fitting in between the frequency range from 119.5 to 120.5 Hz. Figure 3 clearly shows that the higher the number of incoherent integrations the higher the number of answers close to the right value, a well known aspect of using incoherent integrations. An interpretation of this result is to assume that, as we increase the number of spectra in the incoherent integration, we improve the degree of success in estimating the test parameter ( $f_d$ ). However, the application of the technique means longer observational time. For example, in case of to integrate incoherently 10 spectra the observational time is worsened by a factor of 10, i.e., the

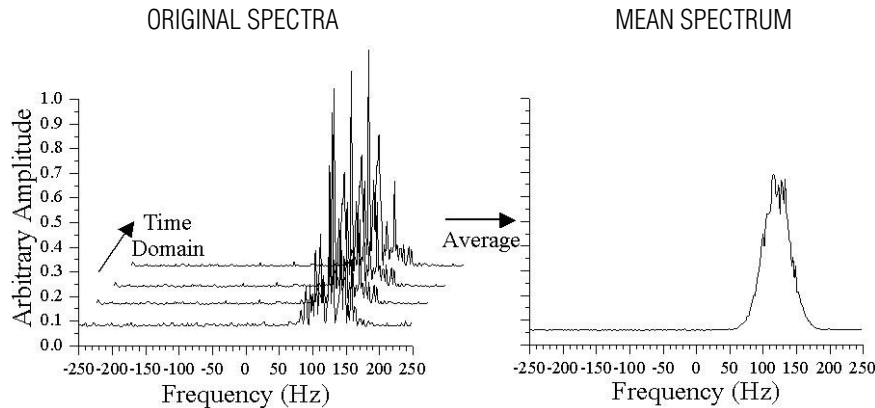


Figure 1 – Illustration of incoherent integration applied to hundred consecutive spectra (left) and the resultant spectrum (right).

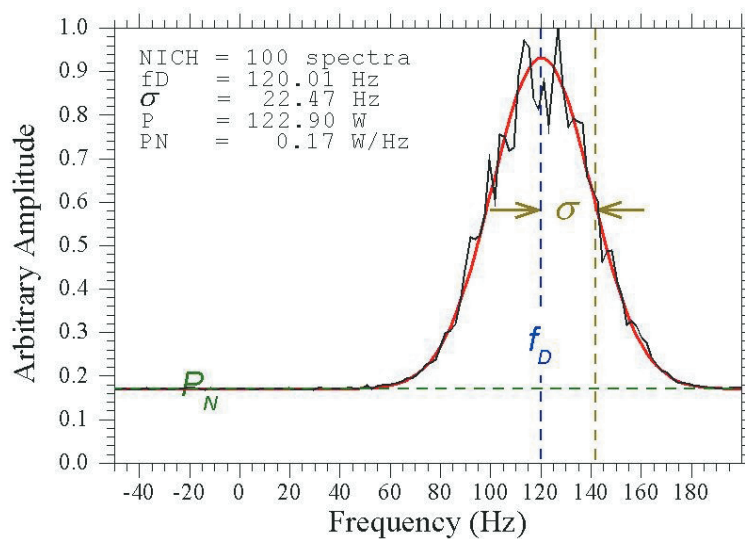


Figure 2 – Power spectrum resulting from the incoherent integration of one hundred simulated power spectra (black line) superimposed by a Gaussian curve (red line) fitted to the spectrum using Least Square Error Method. The green line represents the noise power density ( $P_N$ ), the vertical blue line shows the center of frequency distribution ( $f_d$ ), the difference between the vertical brown and blue lines determines the standard deviation of the Gaussian curve fitted to the spectrum ( $\sigma$ ) and the area between the red and the green line defines the power of the signal ( $P$ ).

observational time increases directly proportional to the number of spectra used in the integration.

The percentage of answers close to the *a priori*  $f_d$  value ( $120 \pm 0.5$  Hz) in function of  $NICH$  is presented in Table 1. The averaged variances of the spectral moments ( $f_d$ ,  $P$  and  $\sigma$ ) estimated from the method and the noise power ( $P_N$ ) obtained by the covariance matrix of the chi-squared distribution (from Eq. 2) are showed in the same table. These results show that the efficiency of the method increased from 9.20% to 99.50%, with a statistical error of 0.42% ( $\pm 0.5$  Hz), when it goes from no incoherent integration ( $NICH = 1$ ) to the incoherent integration of

100 consecutive spectra.

The analysis of the variances of the estimate moments gives us an indication of the accuracy of each parameter for the given SNR (6 dB in the present case). Table 1 shows that the higher the  $NICH$  the lower the variances. A clear example is the high variance of  $\sigma$  when no incoherent integration is applied. This indicates the curve fitting hardly ever have good estimates for this parameter. Our results had shown that increasing  $NICH$  from 1 to 100 spectra results in more than 100 times reduction in the variance of  $f_d$ , which in turn increased the confidence of the Doppler velocity of the plasma irregularity.

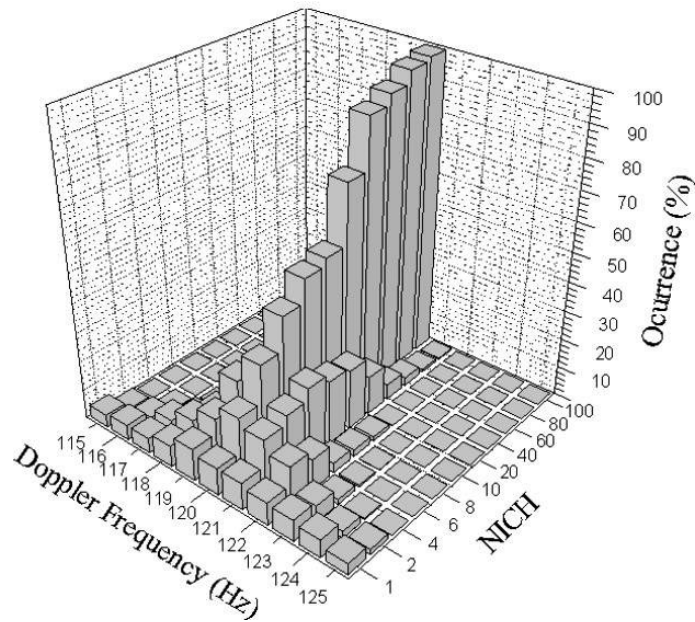


**Figure 3** – Percentage of occurrences of Doppler Frequencies estimated by MLE using spectra with no incoherent integration and integration of 2, 4, 6, 8, 10, 20, 40, 60, 80 and 100 spectra. Each Doppler frequency is centered in the integer frequency defined in the axis with  $\pm 0.5$  Hz of resolution.

**Table 1** – Percentage of answers close to the *a priori*  $f_d$  value ( $120 \pm 0.5$  Hz) in function of *NICH* and the variances of spectral power, Doppler frequency, spectral width and noise.

NICH	Good estimates (%)	Variance of estimate $f_d$ ( $\text{Hz}^2$ )	Variance of estimate $\sigma$ ( $\text{Hz}^2$ )	Variance of estimate $P_N$ ( $10^{-9} \text{ W}^2/\text{Hz}^2$ )	Variance of estimate $P$ ( $10^{-6} \text{ W}^2$ )
1	9.20	4.6455	12.1841	18.527	4.8421
2	20.70	2.0206	0.9342	22.205	4.2802
4	33.20	0.9588	0.4389	15.841	2.8436
6	44.30	0.6303	0.2877	11.812	2.0767
8	52.00	0.4689	0.2142	9.342	1.6248
10	54.40	0.3738	0.1707	7.707	1.3311
20	74.20	0.1857	0.0849	4.090	0.7025
40	90.80	0.0927	0.0424	2.112	0.3596
60	94.20	0.0617	0.0282	1.422	0.2414
80	98.30	0.0462	0.0211	1.072	0.1824
100	99.50	0.0370	0.0169	0.859	0.1460

The last two parameters of Table 1 indicate good results after incoherent integration. The variance of estimate  $P_N$  reduces itself more than 20 times increasing *NICH* from 1 to 100 spectra. It means that the white noise level is better defined, separating that one from the information of the Gaussian curve. Table 1 still shows that the variance of estimate  $P$  is more than 30 times better determined after 100 spectra incoherent integrations. It indicates

a better definition of the intensity of the turbulence, since they are proportional to each other.

The graph of Figure 4 shows the mathematical relationship between the number of integrated spectra and the number of occurrences close to the *a priori*  $f_d$  value ( $120 \pm 0.5$  Hz). The dots give the Percentage of Right Estimated Answers (*PREA*) for  $f_d$  as a function of the number incoherent integrations. The line

named saturation marks the maximum possible value of percentage, i.e., 100% of occurrences. This figure clearly shows a logarithmic dependence of the percentage of right answers from the number of incoherent integrations. In order to quantify this relation, we have performed a linear fitting like logarithmic growth on this data, represented by the curve superimposed to the Figure 4. The following equation has been used for this fitting:

$$PREA = \alpha \cdot \ln(NICH) + \beta, \quad (4)$$

$$1 \leq NICH \leq 100,$$

where *PREA* is the Percentage of Right Estimated Answers,  $\alpha$  could be considered as a growing rate of *PREA* and  $\beta$  is the *PREA* observed when no incoherent integrations is applied to the data set. The fitting resulted an  $\alpha = 21.01 \pm 0.66$  and a  $\beta = 7.46 \pm 1.93$ , with a quadratic correlation factor as  $R^2 = 0.9912$ . The points with lower *NICH* are better fitted than the higher ones because the points are closer to each other for lower *NICH* (2, 4, 6, 8 and 10) than for higher *NICH* (20, 40, 60, 80 and 100). Despite the logarithmic growing (curve of Fig. 4) did not fit perfectly to the data (dots) at high *NICH* values, we have obtained a quadratic correlation factor higher than 99%. Moreover, we expect a better fitting of the logarithmic growing curve for *NICH* higher than 100. The step that the good estimates increases as we increase the number of incoherent integrations is also an interesting result. For instance, when the *NICH* is increased from 60 to 100 the *PREA* differs in less than 6%, but the observational time increases by almost 66%. This indicates there should be some optimal point above of which increases in the *NICH* do not substantially improve the *PREA* without compromise the observational time. Finally, this results show that in case of using incoherent integration one must choose the lowest number of incoherent integration as possible, i.e., before the asymptotic region in the logarithmic law (Eq. 4). We should also remember that Eq. (4) is a result of the analysis from simulated data and we may obtain higher or lower values of standard deviation of the noise ( $\sigma_N$ ) in a case of real spectra of radar. So, in spite of Eq. (4) does not give a description for real cases, it is expected that the logarithmic characteristic between *PREA* and *NICH* remains valid, being helpful to a qualitative analysis.

Other point we would like to address in this paper is the dependence of the averaged variance of  $f_d(VAR_{FD})$  from the number of integrated spectra (*NICH*). Figure 5 presents the mathematical relationship between the averaged variance (dots) and the number of incoherent integration. The graph clearly shows a linear dependence between the natural logarithmic of variance

of  $f_d$  and the natural logarithmic of the incoherent integrations. In order to quantify the dependence, we have performed a linear fitting to these data in ln-ln domain, represented by the curve superimposed to the graph on Figure 5. The following equation has been used to fit the data:

$$VAR_{fd} = NICH^\varepsilon \cdot e^\psi, \quad (5)$$

$$1 \leq NICH \leq 100,$$

where  $VAR_{fd}$  is the fitted variance of estimate  $f_d$ ,  $\varepsilon$  is the negative power coefficient that tell us how much the  $VAR_{fd}$  reduces as we increase the *NICH*, and the exponential of  $\psi$  is the  $VAR_{fd}$  observed when no incoherent integration is applied. The power coefficient  $\varepsilon$  resulted  $-1.0341 (\pm 0.00954)$ . The  $\psi$  factor resulted  $1.43189 (\pm 0.02804)$ . And the correlation factor *R* resulted  $-0.99962$ . Observe that the negative power coefficient is very close to the unit. This indicates that increases in the number of spectra incoherently integrated will almost proportionally decrease the variance of the estimate Doppler frequency. Also, when no incoherent integration is applied the power coefficient effect will be negligible. And the variance will be given by the exponential of  $\psi$  factor. Therefore, Eq. (5) in this simple form seems to give a comprehensive idea of how the variance will behave as we apply incoherent integrations to our data set. Higher values of *NICH* will proportionally reduce the variance of the estimate Doppler frequency. On the other hand, it will also proportionally increase the observational time. Consequently, the compromise of the observational time seems to be linear related to the increase of the number of incoherent integration and to the decrease of the variance. Moreover, the  $\psi$  factor seems to be related to SNR of the data set. Reductions in to the SNR will probably reduce  $\psi$  factor. Hence, this factor should be related to noise level on the radar system.

Finally, applying incoherent integrations to the observational radar spectra of type 1 equatorial electrojet irregularities means a compromise among the percentage of right estimated answers when using MLE techniques for estimating the Doppler frequency, the variance of the estimate Doppler frequency and the observational time. For the present study we have observed that small numbers of incoherent integrations decreases substantially the variance of the estimate Doppler frequency as well as increases the percentage of right estimated answers, without much compromise to the observational time. Larger number of incoherent integrations will fall into the asymptotic region of the *PREA* curve and will not significantly decreases the variance of the estimate Doppler frequency, but will considerably compromise the observational time.

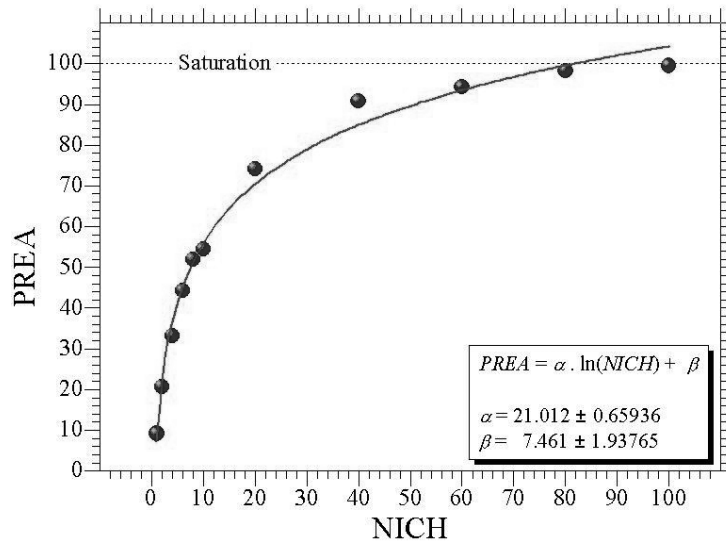


**Figure 4** – Percentage of right estimated answers ( $PREA$ ) in function of the number spectra used in the incoherent integrations ( $NICH$ ). The analyzed incoherent integrations are the dots and the logarithmical fitting is the curve. The dashed line shows the saturation of  $PREA$ , i.e., 100% of occurrences.

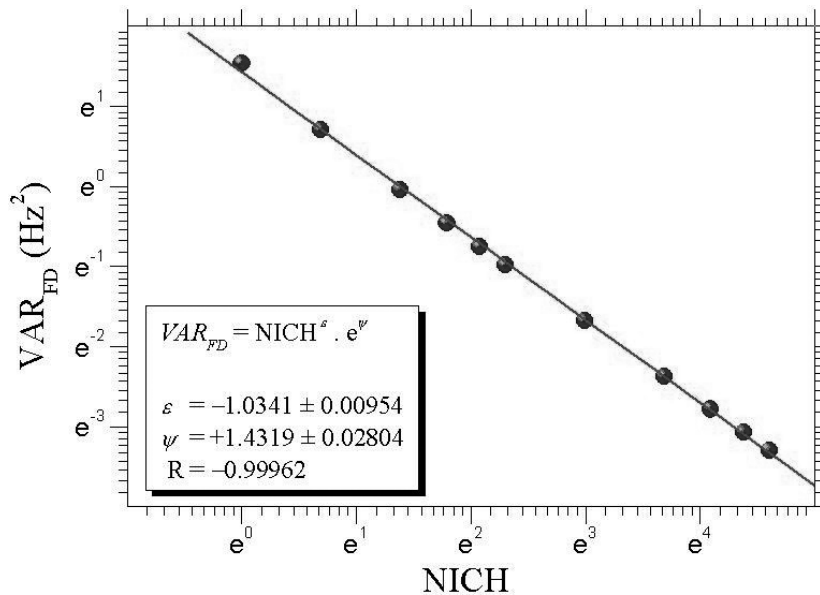


**Figure 5** – Averaged variance of  $f_d$  associated with the fitting method ( $VAR_{FD}$ ) in function of the number spectra used in the incoherent integrations ( $NICH$ ). The analyzed incoherent integrations are the dots and the logarithmical fitting is the curve.

## CONCLUSIONS

The technique of incoherent integration has shown to be a valuable tool, which is able to improve significantly the estimates of the test parameter (the center of the frequency distribution of the power spectra from the radar echoes of the EEJ irregularities).

As a result of increasing the number of incoherently integrated spectra, the degree of success in estimating the test parameter is improved. We have shown a logarithmic growth dependence of the percentage of right estimate answers from the number of incoherent integrations, and this mathematical relationship has been quantified through a linear fitting. We have also addressed

in this paper the linear dependence of the natural logarithmic of variance of the estimate  $f_d$  and the natural logarithmic of the incoherent integration. The power coefficient  $\varepsilon$  from linear fitting indicated that increases in the number of spectra incoherently integrated will almost proportionally decrease the variance of the estimate Doppler frequency. In addition, we have found an exponential factor  $\psi$ , which we believe to be related to SNR of the data set. Reducing the SNR will probably reduce this factor. Finally, we have seen that applying incoherent integrations to the observational radar spectra of type 1 equatorial electrojet irregularities means to increase the percentage of right estimated answers when using MLE techniques for estimating the Doppler frequency, but we have to balance the variance of the estimate Doppler frequency and the observational time.

### ACKNOWLEDGMENTS

The first author wishes to thank CNPq/MCT for financial support to his undergraduate program through the project 107616/2003-3. The second author wishes to thank FAPESP (2005/01113-7) for the financial support to attend the 9th CISBGf in which congress this work has been presented.

### REFERENCES

- ABDU MA, DENARDINI CM, SOBRAL JHA, BATISTA IS, MURALI-KRISHNA P & DE PAULA ER. 2002. Equatorial electrojet irregularities investigations using a 50 MHz back-scatter radar and a Digisonde at São Luís. *Journal of Atmospheric and Solar-Terrestrial Physics*, 64(12-14): 1425–1434.
- ABDU MA, DENARDINI CM, SOBRAL JHA, BATISTA IS, MURALI-KRISHNA P, IYER KN, VELIZ O & DE PAULA ER. 2003. Equatorial electrojet 3 m irregularity dynamics during magnetic disturbances over Brazil: results from the new VHF radar at São Luís. *Journal of Atmospheric and Solar-Terrestrial Physics*, 65(14-15): 1293–1308.
- BALSLEY BB. 1969. Some Characteristics of Non-2-Stream Irregularities in Equatorial Electrojet. *Journal of Geophysical Research*, 74: 2333–2347.
- BUNEMAN O. 1963. Excitation of field aligned sound waves by electron streams. *Physical Review Letters*, 10(7): 285–287.
- COHEN R & BOWLES KL. 1967. Secondary Irregularities in Equatorial Electrojet. *Journal of Geophysical Research*, 72: 885–894.
- COHEN R. 1973. Phase Velocities of Irregularities in Equatorial Electrojet. *Journal of Geophysical Research*, 78: 2222–2231.
- DE PAULA ER & HYSELL DL. 2004. The São Luís 30 MHz coherent scatter ionospheric radar. System description and initial results. *Radio Science*, 39(1): 1–11.
- DENARDINI CM, ABDU MA & SOBRAL JHA. 2004. VHF radar studies of the equatorial electrojet 3-m irregularities over São Luís: day-to-day variabilities under auroral activity and quiet conditions. *Journal of Atmospheric and Solar-Terrestrial Physics*, 66(17): 1603–1613.
- DENARDINI CM, ABDU MA, DE PAULA ER, SOBRAL JHA & WRASSE CM. 2005. Seasonal characterization of the equatorial electrojet height rise over Brazil as observed by the RESCO 50 MHz back-scatter radar. *Journal of Atmospheric and Solar-Terrestrial Physics*, 67(17-18): 1665–1673.
- FARLEY DT. 1963. A plasma instability resulting in field aligned irregularities in the ionosphere. *Journal of Geophysical Research*, 68(A22): 6083–6097.
- FARLEY DT. 1985. Theory of equatorial electrojet plasma waves: new developments and current status. *Journal of Atmospheric and Terrestrial Physics*, 47(8-10): 729–744.
- FEJER BG, FARLEY DT, BALSLEY BB & WOODMAN RF. 1975. Vertical Structure of VHF Backscattering Region in Equatorial Electrojet and Gradient Drift Instability. *Journal of Geophysical Research*, 80: 1313–1324.
- FEJER BG & KELLEY MC. 1980. Ionospheric Irregularities: Reviews of Geophysics and Space Physics, 18(2): 401–454.
- FORBES JM. 1981. The Equatorial Electrojet: Reviews of Geophysics and Space Physics, 19(3): 469–504.
- FUKAO S. 1989. Middle atmosphere program – Handbook for map: International school on atmospheric radar, Vol. 30, Urbana (IL): SCOSTEP Secretariat. 364 pp.
- LEVENBERG K. 1944. A Method for Solution of Certain Non-Linear Problems in Last Squares. *Quarterly of Applied Mathematics*, 2(1): 164–168.
- MARQUARDT DW. 1963. An Algorithm for Least-Squares Estimation of Nonlinear Parameters. *Journal of the Society for Industrial and Applied Mathematics*, 11(2): 431–441.
- MAY PT & STRAUCH RG. 1989. An Examination of Wind Profiler Signal Processing Algorithms. *Journal of Atmospheric and Oceanic Technologies*, 6(4): 731–735.
- MAY PT, SATO T, YAMAMOTO M, KATO S, TSUDA T & FUKAO S. 1989. Errors in the Determination of Wind Speed by Doppler Radar. *Journal of Atmospheric and Oceanic Technologies*, 6(2): 235–242.
- PRAKASH S, GUPTA SP, SUBBARAY BH & JAIN CL. 1971. Electrostatic Plasma Instabilities in Equatorial Electrojet. *Nature (Physical Science)*, 233(38): 56–58.
- PRESS WH, TEUKOLSKY SA, VETTERLING WT & FLANNERY BP. 1992. *Numerical recipes in C: the art of scientific computing*. 2. ed. Cambridge: Cambridge University Press. 994 pp.



- REDDY CA. 1981. The equatorial electrojet: a review of ionospheric and geomagnetic aspects. *Journal of Atmospheric and Terrestrial Physics*, 43(5/6): 557–571.
- REDDY CA & DEVASIA CV. 1981. Height and Latitude Structure of Electric-Fields and Currents Due to Local East-West Winds in the Equatorial Electrojet. *Journal of Geophysical Research*, 6: 5751–5767.
- ROGISTER A & D'ANGELO N. 1970. Type II irregularities in the equatorial electrojet. *Journal of Geophysical Research*, 75: 3879–3887.
- SOMAYAJULU VV. 1991. Ionospheric Irregularities and Plasma Instabilities, in *First Winter School on Indian MST Radar*, edited by K.S. Krishnan Marg, Publications & Information Directorate, Sri Venkateswara University, Tirupati – India. 151 pp.
- WOODMAN RF. 1985. Spectral moment estimation in MST radars. *Radio Science*, 20(6): 1185–1195.
- ZRNIC DS. 1979. Estimation of spectral moments of weather echoes. *IEEE Transactions of Geoscience on Electronics*, 17: 113–128.

## NOTES ABOUT THE AUTHORS

**Henrique Carlotto Aveiro**, cited as AVEIRO HC, is Technician in Telecommunications formed at Centro Federal de Educação Tecnológica de Pelotas, CEFET-RS, in 2001. He earned his Electrical Engineering degree in 2007 at the Universidade Federal de Santa Maria (UFSM). He has worked with research in Aeronomy, with special focus on ionospheric radar signal processing and equatorial ionospheric studies. In 2005 he received the Young Scientist Award from International Union of Radio Science, URSI. Nowadays, he is Master Student of Space Geophysics at INPE/MCT and member of the group of researchers and engineers of the Aeronomy Division at INPE/MCT.

**Clezio Marcos Denardini**, cited as DENARDINI CM, earned his electrical engineering degree in 1996 at the Universidade Federal de Santa Maria (UFSM) and his Space Science Ph.D in 2003 at the National Institute for Space Research (INPE), where he is currently working as a researcher. His major field is Space Geophysics with focus in the Equatorial Aeronomy in which he had advised Master and Undergraduate scientific projects. He had published 9 international articles in indexed journals and presented 58 reports in scientific events. He had developed 1 technological product and 3 softwares. He had participated in the international cooperation among INPE, the Air Force Philips Laboratory (AFPL) and the UFSM (INPE/AFPL/UFSM). He had earned 2 scientific awards.

**Mangalathayil Ali Abdu**, cited as ABDU MA, is graduated in Physics at the Kerala University, India in 1959; Msc. in Electronics and Physics in 1961 at the Kerala University, and Ph.D. in 1967, in Aeronomy at the Gujarat University, India. The doctorate research was developed in the department of space research at Physical Research Laboratory, Ahmedabad. Post-Doc in the department of physics at Western Ontario University, Canada, where he worked in development of ionospheric studies techniques by meteor trails. He was P.I. by projects funded by IAGA (International Association of Geomagnetism and Aeronomy) and SCOSTEP (Scientific Committee on Solar-Terrestrial Physics). He is assessorate of FAPESP, CNPq, NSF and NASA. Nowadays he is Titular Researcher at INPE in dynamics of the ionosphere-thermosphere-magnetosphere-interplanetary medium system by radiofrequency and optical methods.

**Nelson Jorge Schuch**, cited as SCHUCH NJ, is graduated in Physics at the Federal University of Santa Maria – UFSM, in 1972. M.Sc. (Physics) – Extra Galactic Astrophysics, University of Mackenzie, São Paulo, Brazil, in 1975. Ph.D. (Astrophysics) – University of Cambridge, Cambridge, England, in 1979. Post Doctoral Experience at Cambridge University, England, in 1979/1980. From 1980 to 1995, he worked as Senior Researcher/Vice-Director of the National Observatory – ON/MCT, in Rio de Janeiro. In 1996 he was named Coordinator of the Radioastronomy Project – RA, in the Partnership between INPE/MCT – UFSM. Nowadays he is the Head of the Southern Regional Space Research Center, from the National Institute for Space Research, INPE/MCT's Unit in Santa Maria, with its subunit the Southern Space Observatory – OES/CRSPE/INPE – MCT, in São Martinho da Serra, RS. He works in the field of Astrophysics, with emphasis in Radioastronomy/Observational Cosmology, and also on Space and Atmospheric Sciences, with emphasis in the Earth-Sun Interactions, Space Weather, Aeronomy, Space Geophysics. In his professional activities, interacted with many collaborators, with more than 669 publications.